Proceedings of the 11th Brazilian Congress of Thermal Sciences and Engineering – ENCIT 2006
Braz. Soc. of Mechanical Sciences and Engineering – ABCM, Curitiba, Brazil, Dec. 5-8, 2006

Paper CIT06-0271

ADVANCED EDDY-VISCOSITY AND REYNOLDS-STRESS TURBULENCE MODELS FOR AEROSPACE FLOWS

Enda Dimitri V. Bigarella
Instituto Tecnológico de Aeronáutica, CTA/ITA, São José dos Campos, BRAZIL
enda.bigarella@gmail.com

João Luiz F. Azevedo
Instituto de Aeronáutica e Espaço, CTA/IAE, São José dos Campos, BRAZIL
azevedo@iae.cta.br

Abstract. *Recent improvements on a 3-D unstructured-mesh finite-volume method for complex aerospace applications are presented. The correct modelling of turbulence effects in aerospace flows is paramount for their successful computation. One-equation and two-equation models based on the linear approximation of the Boussinesq hypothesis are used. The linear approximation is also extended to include a nonlinear formulation resulting from an explicit algebraic Reynolds-stress model. Finally, two Reynolds-stress closures are also available. Both nonlinear eddy-viscosity and Reynolds-stress model formulations naturally offer the potential for more reliable predictions than linear approximations since anisotropy of the Reynolds stresses can be accounted for. Experimental and DNS results are used for verification and validation of the turbulence model implementation. Focus is directed towards the effect of anisotropy for the resolution of the interaction between shock wave and boundary layers. In general, good agreement with theoretical or experimental results is obtained.*

keywords: *CFD, Turbulence model, Aerospace flows.*

1. Introduction

The present paper reports on recent improvements on a 3-D unstructured-mesh finite-volume method for complex aerospace applications developed by the CFD group at Instituto de Aeronáutica e Espaço (IAE). The objective of the CFD group at IAE is to develop the capability of simulating 3-D, viscous turbulent flows over general launch vehicle configurations. Viscous simulations at high Reynolds numbers are typical for aerospace applications, such as the ones of interest to IAE, and turbulence is certainly important for these flow regimes. The correct modelling of turbulence effects in aerospace flows is decisive for consistent computation of complex phenomena such as boundary layers subjected to adverse-pressure gradients, boundary-layer/shock-wave interactions, wing wakes, mixing layers, and others.

The current code has already been used to simulate turbulent viscous flows over typical aerospace configurations with linear eddy-viscosity turbulence models (EVMs), with successful results so far (Bigarella *et al.*, 2004). For such effort, the Spalart and Allmaras, 1994, one-equation and the Menter, 1994, SST two-equation turbulence models have been chosen. Further extension of the code included the realisable k-ϵ (Shih *et al.*, 1994) and the low-Reynolds-number k-ω (Fluent, 1998) models. The linear approximation resulting from the Boussinesq hypothesis, used by the previous models, is currently extended to include a nonlinear formulation resulting from the explicit algebraic Reynolds-stress model (EARSM) of Wallin and Johansson, 2000. The nonlinear formulation allows for better capture of normal stress and streamline curvature effects, which are important for the already mentioned flow phenomena.

For completeness of the modelling effort, two Reynolds-stress models (RSMs) are also included. Their formulation naturally offers the potential for more reliable prediction of the aforementioned turbulence effects, since important terms are exactly treated. The high-Reynolds number Menter StressBSL uses a linear approximation for the pressure correlation term and an isotropic approximation to the turbulent dissipation. The more advanced Craft-Launder RSM (Batten *et al.*, 1999) is a low-Reynolds number closure, with an anisotropic representation of the turbulent dissipation, and a cubic model for the pressure correlation term.

Extensive validation of this code had already been initiated (Scalabrin, 2002; Bigarella *et al.*, 2004; Bigarella and Azevedo, 2005). Currently, turbulence models are validated for a parallel-wall channel flow case. Numerical results are compared to DNS results. Further results are presented for transonic flows over a supercritical aerofoil. Simulation results are compared to available wind-tunnel experimental data. In general, acceptable numerical results are obtained.

2. Theoretical Formulation

2.1. RANS Equations

The flows of interest in the present context are modelled by the 3-D compressible Reynolds-averaged Navier-Stokes (RANS) equations (Scalabrin, 2002), written in dimensionless form and assuming a perfect gas, as

$$\frac{\partial \mathbf{Q}}{\partial t} + \nabla \cdot (\mathbf{P}_e - \mathbf{P}_v) = 0 \ , \qquad \mathbf{Q} = \left[\ \rho \quad \rho\, u \quad \rho\, v \quad \rho\, w \quad e \ \right]^{\mathrm{T}} \ , \tag{1}$$

where $\mathbf{Q}$ is the dimensionless vector of conserved variables, ρ is the fluid density, $\mathbf{v} = \{u, v, w\}$ is the Cartesian velocity vector and e is the fluid total energy per unit of volume. The inviscid flux vector, $\mathbf{P}_e$, and the viscous flux vector, $\mathbf{P}_v$, are given as

$$\mathbf{P}_e = \left\{ \begin{array}{c} \rho\,\mathbf{v} \\ \rho\, u\mathbf{v} + p\,\hat{\imath}_x \\ \rho\, v\mathbf{v} + p\,\hat{\imath}_y \\ \rho\, w\mathbf{v} + p\,\hat{\imath}_z \\ (e+p)\,\mathbf{v} \end{array} \right\} \ , \quad \mathbf{P}_v = \frac{1}{Re} \left\{ \begin{array}{c} 0 \\ \left(\tau^{\ell}_{xi} + \tau^{t}_{xi}\right)\,\hat{\imath}_i \\ \left(\tau^{\ell}_{yi} + \tau^{t}_{yi}\right)\,\hat{\imath}_i \\ \left(\tau^{\ell}_{zi} + \tau^{t}_{zi}\right)\,\hat{\imath}_i \\ \beta_i\,\hat{\imath}_i \end{array} \right\} \ , \tag{2}$$

where $i = x$, y or z are the indices used within the Einstein indexing notation; and $\hat{\imath} = \{\hat{\imath}_x, \hat{\imath}_y, \hat{\imath}_z\}$ is the Cartesian coordinate unit vector. Furthermore, τ^{ℓ}_{ij} is the shear-stress tensor, u_i is the Cartesian velocity component, x_i is the Cartesian coordinate, δ_{ij} is the Kronecker delta, and $\beta_i = \tau^{\ell}_{ij} u_j + q_i$, where q_i is the heat transfer vector Cartesian component. The dimensionless pressure, p, can be calculated from the perfect gas equation of state.

This set of equations is solved according to a finite volume formulation (Scalabrin, 2002). For convective-flux calculations on the volume faces, the Roe, 1981, flux-difference splitting scheme is currently used. In order to achieve 2nd-order of accuracy in space, properties are linearly reconstructed in the faces based on the van Leer, 1979, MUSCL algorithm. The implementation follows a modified and generalised Barth and Jespersen, 1989, multidimensional limiter formulation from Bigarella and Azevedo, 2005. Diffusive-flux terms are discretized based on a usual centred scheme, with properties in the faces obtained as an arithmetical average of the properties in the neighbouring cells. Flow equations are integrated in time by a fully explicit, 2nd-order accurate, 5-stage, Runge-Kutta time stepping scheme. An agglomeration full-multigrid scheme (FMG) is included in order to achieve better convergence rates for the simulations. More details on the theoretical and numerical formulations can be found in Bigarella *et al.*, 2004, and Bigarella and Azevedo, 2005.

2.2. Turbulence Modelling

High-Reynolds number simulations of flows over complex aerodynamic configurations require adequate turbulence closures in order to correctly account for the large transport effects of the turbulence at such flight conditions. The turbulence effects are included into the RANS equations by the Reynolds-stress tensor, defined by $\tau^{t}_{ij} = -Re\rho\overline{u_i'' u_j''}$. The model transport equations are also solved according to the finite volume approach. The time march is performed using the implicit Euler scheme as in Scalabrin, 2002. For the discretization of the advection term a 1st-order upwind scheme is used, in order to avoid oscillations near discontinuities. For the discretization of the diffusion term an alternative method to compute non-oscillatory derivatives in the face is used as an approximate finite difference scheme. This approximation uses the adjacent cell centroid property and relative distance to build the derivative in the face. More details can be found in Bigarella and Azevedo, 2006.

3. Eddy-Viscosity Turbulence Models

Eddy viscosity models compute the Reynolds stresses through the Boussinesq hypothesis, which states that the turbulence stresses are a linear function of the mean flow straining rate times a modifying constant such as

$$\tau^{t}_{ij} = \mu_t \left[\left(\frac{\partial u_i}{\partial x_j} + \frac{\partial u_j}{\partial x_i} \right) - \frac{2}{3} \frac{\partial u_m}{\partial x_m} \delta_{ij} \right] - \frac{2}{3} \rho k\, \delta_{ij} \ , \tag{3}$$

where μ_t is the eddy viscosity coefficient, computed by the chosen turbulence model.

3.1. Spalart-Allmaras (SA) Model

The Spalart and Allmaras, 1994, single equation model solves a transport equation for the modified eddy viscosity coefficient $\tilde{\mu}$. This models is derived along intuitive and empirical lines, relying heavily on calibration

by reference to a wide range of experimental data (Spalart and Allmaras, 1994). It can be easily integrated to the wall for meshes that guarantee $y+ \approx 1$ close to the wall. This same model has been applied without any further modification by the CFD community for 3-D compressible flows with good results so far (Spalart, 2000; Leschziner and Drikakis, 2002) in shock-induced separations and adverse pressure gradient boundary layers.

3.2. Low-Reynolds-Number Wilcox k-ω (WKOM) Model

The k-ω model is an empirical closure based on transport equations for k and ω (Wilcox, 1998). This model is constantly evolving over the years, including corrections and improvements to a wide range of different flow cases. A low-Reynolds number version of the k-ω model, also enhanced for improved accuracy in free shear flows, from Fluent, 1998, is currently used. The model is closed with constants (Fluent, 1998) obtained from calibration against key test cases for turbulent flows (Wilcox, 1998). This model can also be integrated to the wall.

3.3. Realisable k-ϵ (RKE) Model

The realisable k-ϵ model from Shih *et al.*, 1994, solves transport equations for k and ϵ. Differently from a standard k-ϵ model (Jones and Launder, 1972), this model employs in the dissipation-rate equation a realisable estimate of the turbulent time scale, and an additional term developed to improve the model response to adverse-pressure gradient regions, to guarantee acceptable model behaviour. Furthermore, the eddy viscosity coefficient is defined for this model as a function of the local flow straining in order to also increase the model realisability and response to adverse pressure gradients. A low-Reynolds number damping function, designed to account for the damping of turbulent fluctuations near solid walls, is also considered in the eddy viscosity definition. These enhancements render this model robust and consistent behaviour near solid walls, and better response to pressure gradients.

3.4. Shear-Stress Transport (SST) Model

The Menter, 1994, SST model is derived from a blend of the original k-ω (Wilcox, 1998) and the standard k-ϵ (Jones and Launder, 1972) models. It solves reported problems of the k-ω closure regarding freestream value dependency (Menter, 1994) while keeping the better numerical behaviour of this model close to the wall. Model constants are generally calculated as $\phi = F_1\phi_1 + (1 - F_1)\phi_2$, where ϕ_1 represents the set of constants for the k-ω model and ϕ_2, the set for the standard k-ϵ model (Menter, 1994). The F_1 variable is a blending function that turns on the k-ω closure near solid walls and the standard k-ϵ model outside boundary layers. This function is computed based on checks over turbulence properties through the boundary layer.

Standard two-equation models are acknowledged for not being capable of accurately computing adverse pressure gradient or separated flows (Menter, 1994). It is demonstrated that this is a result of the missing effect of turbulent shear-stress transport in this type of flow (Johnson and King, 1985). In order to take this shear-stress into account, at least in an ad-hoc fashion, the eddy viscosity coefficient is here constrained by the magnitude of the shear-stress tensor. This limiting comes from the knowledge that the shear stress inside the boundary layer is proportional to k as $\tau_{ij}^t = a_1\rho k$ for $i \neq j$, and that, in adverse pressure gradient regions, the Boussinesq assumption $\tau_{ij}^t = 2\mu_t S$ is known to overproduce that term (Menter, 1994). Thus, in such an adverse pressure gradient region, production of k, which is proportional to S, would incorrectly be larger than its dissipation, ω, or $S > a_1\omega$. The SST eddy viscosity coefficient is defined so as to avoid this undesired behaviour. In the simpler BSL model (Menter, 1994), the SST constraint in the eddy viscosity is ignored.

4. Reynolds-Stress Turbulence Models

4.1. General Considerations

Reynolds stress models use the exact equations for the transport of Reynolds stresses obtained by taking velocity-weighted moments of the Navier-Stokes equations and neglecting density fluctuations. The general form of a RSM is given by

$$\frac{D\rho\overline{u_i'' u_j''}}{Dt} = P_{ij} + D_{ij}^{\nu} + D_{ij}^{t} + D_{ij}^{p} + \Phi_{ij}^{*} - \epsilon_{ij} \ , \tag{4}$$

with the individual terms representing specific turbulence mechanisms, where P_{ij} is the turbulent production; D_{ij}^{ν} is the molecular diffusion; D_{ij}^{t} is the turbulent diffusion; D_{ij}^{p} is the pressure diffusion; Φ_{ij}^{*} is the pressure-strain correlation; and ϵ_{ij} is the turbulent dissipation. The turbulent production and the molecular diffusion

terms do not require modelling. The representation of the remaining terms is model dependent and they are discussed separately in the respective following subsections.

RSMs also require the solution of another transport equation for a measure of the turbulent length scale, usually represented by a turbulent kinetic energy dissipation quantity. The estimation of this quantity is perhaps the weakest point in Reynolds-stress modelling. An exact equation for the dissipation rate can be derived from the Navier-Stokes equations, but this results in a very complicated form. The usual solution is to use an empirically built equation, calibrated against typical turbulence test cases.

4.2. Modified Craft-Launder RSM (CLMRSM)

This RSM is a variation of the nonlinear RSM of Craft and Launder, 1996, which does not require wall-topology parameters such as normal-to-wall vectors and distance from the wall. Modifications of some wall-proximity corrections have been applied to correct the latter model incorrect response to shock waves, which were falsely interpreted as regions of strong inhomogeneity (Batten *et al.*, 1999).

The generalised gradient diffusion hypothesis (GGDH) of Daly and Harlow, 1970, is used for modelling the turbulent diffusion. The pressure diffusion term is also modelled by an empirical approach. Inhomogeneity-indicator vectors are used to indicate regions close to the wall, where turbulence is highly anisotropic. These vectors are based on the Lumley's stress-flatness parameter (Lumley, 1978), which varies between unity in isotropic turbulence regions and zero as the turbulence approaches a two-component limit.

The pressure-strain correlation is considered a critical element for RSMs since it can be of the order of the production and dissipation terms, hence playing a crucial role in most flow cases. Moreover, since it involves correlations which essentially cannot be measured, its modelling requires substantial effort. A cubic pressure-strain model is here used in conjunction with additional coefficients and inhomogeneity corrections. The proposed (Batten *et al.*, 1999) cubic invariant aims at integration through the viscous sublayer and at consistently acting through shock waves, which is an important feature for the flows of interest to IAE.

The dissipation tensor blends isotropic and wall-limiting terms, with an additional term to account for the dip in the shear-stress dissipation rate in the buffer layer. An equation for the homogeneous dissipation rate, ϵ^*, is proposed to determine ϵ. The equation of ϵ^* incorporates a few modifications to better match low-Reynolds number effects near solid walls (Batten *et al.*, 1999). The advantage of using the equation for the homogeneous dissipation rate, ϵ^*, is the simple wall boundary condition $\epsilon^*_{wall} = 0$. Details of this model are given by Batten *et al.*, 1999, and Bigarella and Azevedo, 2006.

4.3. StressBSL RSM

A numerically more robust isotropic turbulence diffusion formulation is chosen for this model. The pressure diffusion, as usual in RSMs, is here neglected. This option uses a linear pressure-correlation model derived from Rotta, 1951 and Launder *et al.*, 1975, along with an isotropic turbulence assumption for the turbulent dissipation tensor. The turbulence-length-scale determining equation is based on the Menter BSL ω equation (Menter, 1994). This set of equations composes a high-Reynolds number turbulence closure. The interested reader is referred to Bigarella and Azevedo, 2006, for thorough details on this model.

4.4. Wallin-Johansson EARSM (NLBSL)

The main motivation in the development of EARSMs is the general need for improvements in the prediction of complicated turbulent flow phenomena using the platform of existing CFD codes based on two-equation eddy-viscosity turbulence modelling capability. This idea represents an interesting way of cheaply incorporating advanced turbulence effects, such as streamline curvature and normal stress separation, into an already existing two-equation turbulence model framework, avoiding thus the large amount of computational resources required by the solution of RSMs.

The classical *algebraic* RSM (ARSM) starts by assuming equilibrium turbulence, which is equivalent to neglecting advection and diffusion in the RSM transport equations. In the formulation of Wallin and Johansson, 2000, the isotropic assumption for the dissipation tensor along with a slight modification of the linear pressure-strain correlations of the StressBSL model are employed. As a result, one gets an implicit algebraic equation for the compressible Reynolds-stress tensor. In the formulation of Wallin and Johansson, 2000, the anisotropy tensor (Bigarella and Azevedo, 2006) is taken instead of the Reynolds-stress tensor, in order to ease the mathematical notation.

The solution of this implicit equation is known to be numerically cumbersome and, thus, a general form for the anisotropy tensor in terms of the shear-stress and rotation tensors is proposed by Wallin and Johansson, 2000. This is the most general form for this tensor rank, composed of ten tensorial independent groups to which all higher-order tensor combinations can be reduced with the aid of the Caley-Hamilton theorem. Each n-th

expansion term is multiplied by a controlling coefficient, β_n, which may be function of independent invariants derived from the shear-stress and rotation tensors. The explicit solution for the anisotropy tensor now relies on the determination of the β_n coefficients. Some researches adopt the approach of calibrating those terms to a set of representative turbulence problems, as Craft *et al.*, 1996. This approach, however, may decrease the generality of the expanded nonlinear terms.

The proposed anisotropy tensor expansion is inserted into the implicit ARSM equation. An explicit algebraic equation for the nonlinear Reynolds stress terms can now be fully determined, as detailed by Wallin and Johansson, 2000. The EARSM is implemented as a plugin to the BSL model. However, the BSL equation was designed in conjunction with a linear constitutive Boussinesq hypothesis. This fact can compromise the performance of the model if rather combined with a nonlinear closure, such as an EARSM (Hellsten, 2005). In order to circumvent these limitations, Hellsten, 2005, proposed a recalibration of the BSL model to make it consistent when augmented with the EARSM nonlinear terms.

5. Results and Discussion

5.1. Initial Remarks

Linear turbulence models are developed considering effects that are essentially linked to the shear stress in the local streamwise direction. Such effects are, for instance, the skin friction or the effect of the boundary layer displacement into the outer irrotational flow. Isotropy of normal stresses is assumed along a streamline because, in a simple shear flow, which usually serves as a calibration milestone for linear EVMs, the normal stresses are dynamically inactive, not contributing to the momentum balance.

The response of the boundary layer to adverse pressure gradient or streamline curvature is, however, dictated by the shear stress as well as the normal stresses. In that case, normal stresses are dynamically active, and they also work towards sensitising the shear stress to the normal straining (as through a shock wave) and curvature. In other words, the shear stress is generated by an interaction between the crossflow normal stress and the local flow straining in such cases. Near the wall, strong anisotropy is found, where the streamwise normal stress is generated by local flow shear straining, and other normal stresses are fed by the redistributive pressure-strain correlation, which tends to steer turbulence towards isotropy. Those aspects emphasise the need for all turbulence models to return realistic levels of anisotropy. These effects are addressed in the test cases to come.

5.2. Fully-Developed Channel Flow

A fully-developed plane-symmetric channel flow DNS experiment as studied by Kim *et al.*, 1987, at friction Reynolds number $Re_\tau = 180$ based on the channel half height, is reproduced with the current numerical code. A grid configuration which supports mesh-independent results, with 90 points along the wall-normal direction and the wall-nearest node located at $y^+ \approx 1$, is used. Reynolds stress tensor components obtained with the present computation and DNS data are plotted in Fig. 1. It is interesting to observe in this figure the already commented fact that the linear EVMs, namely the SA, SST, RKE and WKOM models, predict isotropic normal stress components. In the SA case, the normal stresses are actually zero. The nonlinear augmentation of the NLBSL formulation allows for separation of the normal stresses. Since NLBSL is a high-Reynolds-number closure, the normal stresses close to the wall do not match the actual stress distribution. The same behaviour is found for the StressBSL RSM. Both closures are high-Reynolds-number models and they predict similar Reynolds stresses. The more advanced low-Reynolds-number CLMRSM presents much stronger anisotropy and a very good match with DNS data. Although the streamwise normal stress is underpredicted by this model, this is of no impact in this particular flow because the shear stress is sensitive to the crossflow normal stress, as already discussed. Careful validation of the boundary layer results and additional details can be found in Bigarella and Azevedo, 2006. Although the current Reynolds number may be considered somewhat low, no differences in the models have been found for larger Reynolds number. This is an indication that the models act consistently even for lower Reynolds number flows.

5.3. OAT15A Supercritical Aerofoil

The interaction between shock waves and boundary layers is of considerable practical importance in transonic and supersonic aerospace vehicle design. Strong shock waves may cause massive flow separation leading to early wing stall or other adverse effects. The mechanics of such interactions are complex and poorly understood. However, it is well known that the interaction is highly sensitive to the boundary layer turbulence state, and its response to the deceleration caused by the shock wave. The turbulence field is highly anisotropic in that region and it responds differently under shear, normal or curvature straining. Therefore, there lies the importance

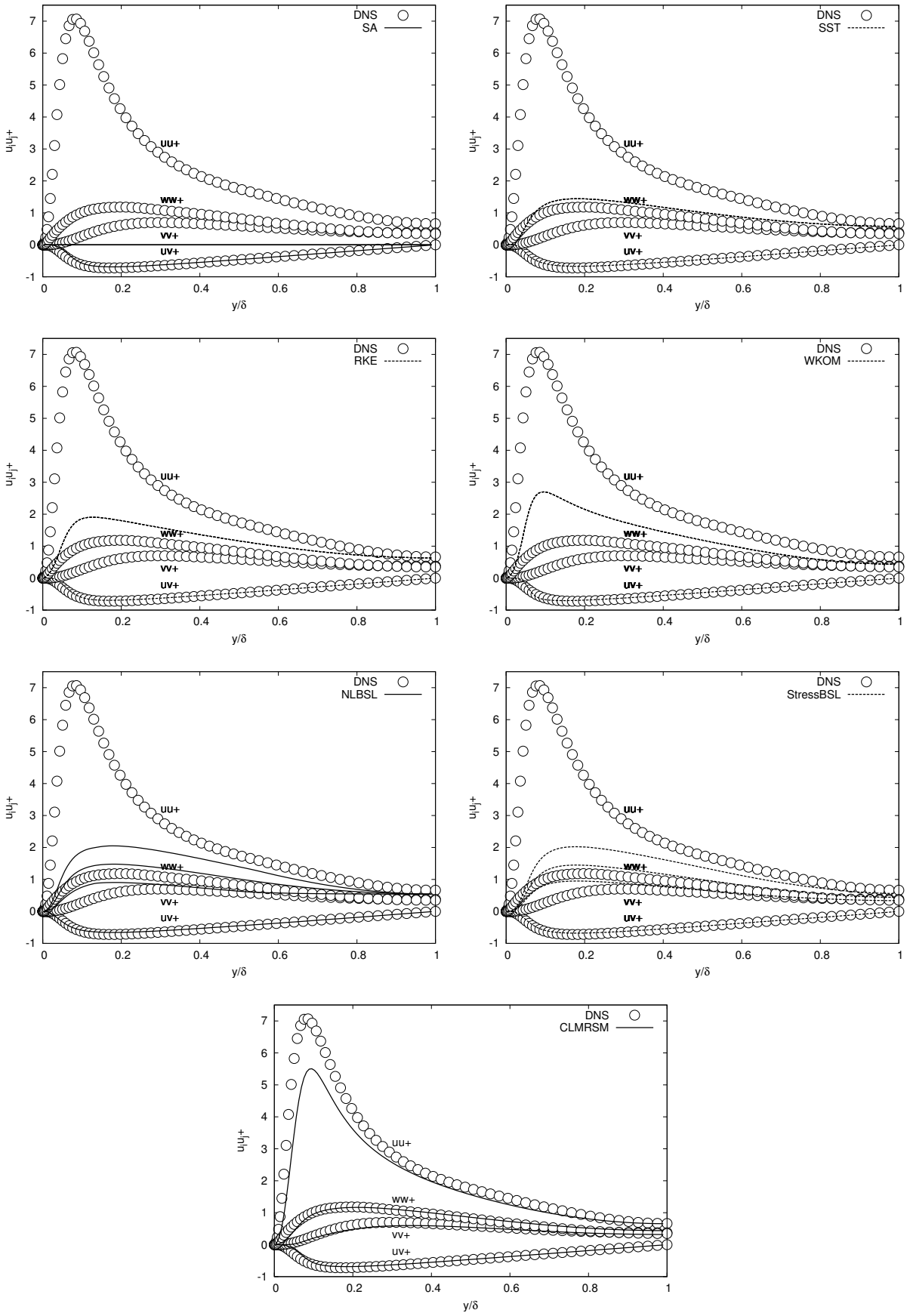

Figure 1: Channel flow at $Re_\tau = 180$. Present computation and DNS Reynolds stresses.

of consistently modelling the turbulence anisotropy and its sensitivity to those types of straining, as earlier discussed.

In order to demonstrate the importance of these remarks, a transonic flow condition over the OAT15A supercritical aerofoil (Rodde and Archambaud, 1994) is addressed. Flight conditions are $M_\infty = 0.724$, $Re = 3$ million, and angle of attack $\alpha = 1.15$ deg. This regime is chosen because the resulting thick boundary layer may more largely interact with the shock wave, being a highly demanding test case for the turbulence models. A grid configuration that is known to support mesh independent results (Bigarella and Azevedo, 2006), with 410 cells along the chord, 34 cells within the boundary layer, and the farfield located 240 chords away, is used. Convergence is considered when the maximum residue of the density field drops 7 orders of magnitude. However, lift and drag coefficients are also monitored to verify force convergence in case density residue would stall.

Numerical pressure coefficient distributions obtained with all turbulence models are compared to the respective experimental data, case 14 in AGARD 303 data (Rodde and Archambaud, 1994), in Fig. 2. It can be clearly seen in this figure the beneficial effects of anisotropy-capable formulation in the turbulence model. All anisotropy-resolving closures, namely NLBSL, StressBSL, and CLMRSM, present good correlation with the experimental result in capturing the shock wave position and the overall pressure distribution. As usual with Boussinesq-based eddy-viscosity models, however, all other linear models indicate a further downstream shock wave location. In the SST case, nevertheless, the eddy viscosity coefficient, limited by the Bradshaw-type constraint, returns a more consistent result among other linear models.

External-probe boundary layer plots at $x/c = 95\%$ for this case are also available. Numerical results are compared to the respective experimental data in Fig. 3. Determining differences are observed in the boundary layer plots in Fig. 3. It is initially seen a strikingly match of the boundary layer obtained with NLBSL and the experimental result. No other model achieves such high accuracy level, in this case. SST, CLMRSM and StressBSL adequately compare to the experimental data, whereas other models present larger differences.

6. Concluding Remarks

The paper presents results obtained with a finite volume code developed to solve the compressible RANS equations. The code uses a Runge-Kutta type scheme to perform time marching. The code is designed to use unstructured meshes composed by any combination of tetrahedra, hexahedra, prisms and pyramids. An agglomeration multigrid scheme provides large convergence acceleration for the numerical simulations. In general, numerical solutions of complicated flows such as transonic turbulent flows about typical aerospace configurations can be obtained in half the previous time used by the single-grid simulation. The convective fluxes are computed by the Roe upwind scheme with MUSCL-type property reconstruction at the faces to achieve 2nd-order of accuracy in space.

Turbulence effects are added to the RANS equations by several advanced turbulence models. The chosen models are specifically designed for aerospace-type flows. The closures range from linear eddy-viscosity, such as the Spallart-Allmaras, SST, realisable k-ϵ, and low-Reynolds-number k-ω models, to nonlinear eddy-viscosity and Reynolds-stress closures. The linear BSL eddy-viscosity formulation is augmented with nonlinear terms coming from an explicit algebraic expansion of a simplified Reynolds-stress equation to compose the NLBSL model. Furthermore, two Reynolds-stress models are also considered. The high-Reynolds-number, linear, and isotropic-dissipation StressBSL model, and the low-Reynolds-number, nonlinear, and anisotropic-dissipation CLMRSM closure are the available Reynolds-stress model options.

Comparison against DNS data for a parallel-wall channel flow case shows the levels of turbulence representativeness that is obtained with each modelling approach. Differences are observed when anisotropy is considered. In these cases, separation of normal stresses can be observed. The code is also able to correctly solve for complex flows, such as the transonic turbulent flow about a supercritical aerofoil. In this case, it is observed that the correct modelling of the turbulence effects inside the boundary layer, mainly regarding the anisotropy of the normal stresses, is of paramount importance for the successful computation of shock wave/boundary layer flows. The NLBSL model presents a large advantage over the other currently considered options since it returns much higher accurate results than other models at computational costs similar to those of a standard two-equation model. The results presented here are a good indication of the capability of simulating turbulent flows about relevant aerospace geometries that can be achieved with the present numerical tool.

7. Acknowledgements

The authors would like to acknowledge Conselho Nacional de Desenvolvimento Científico e Tecnológico, CNPq, which partially supported the project under the Integrated Project Research Grant No. 501200/2003-7. The authors also acknowledge Dr. P. Batten of Metacomp Technologies, USA, and Dr. S. Wallin at Linköping University, Sweden, for their insights on specifics of the respective turbulence model implementations.

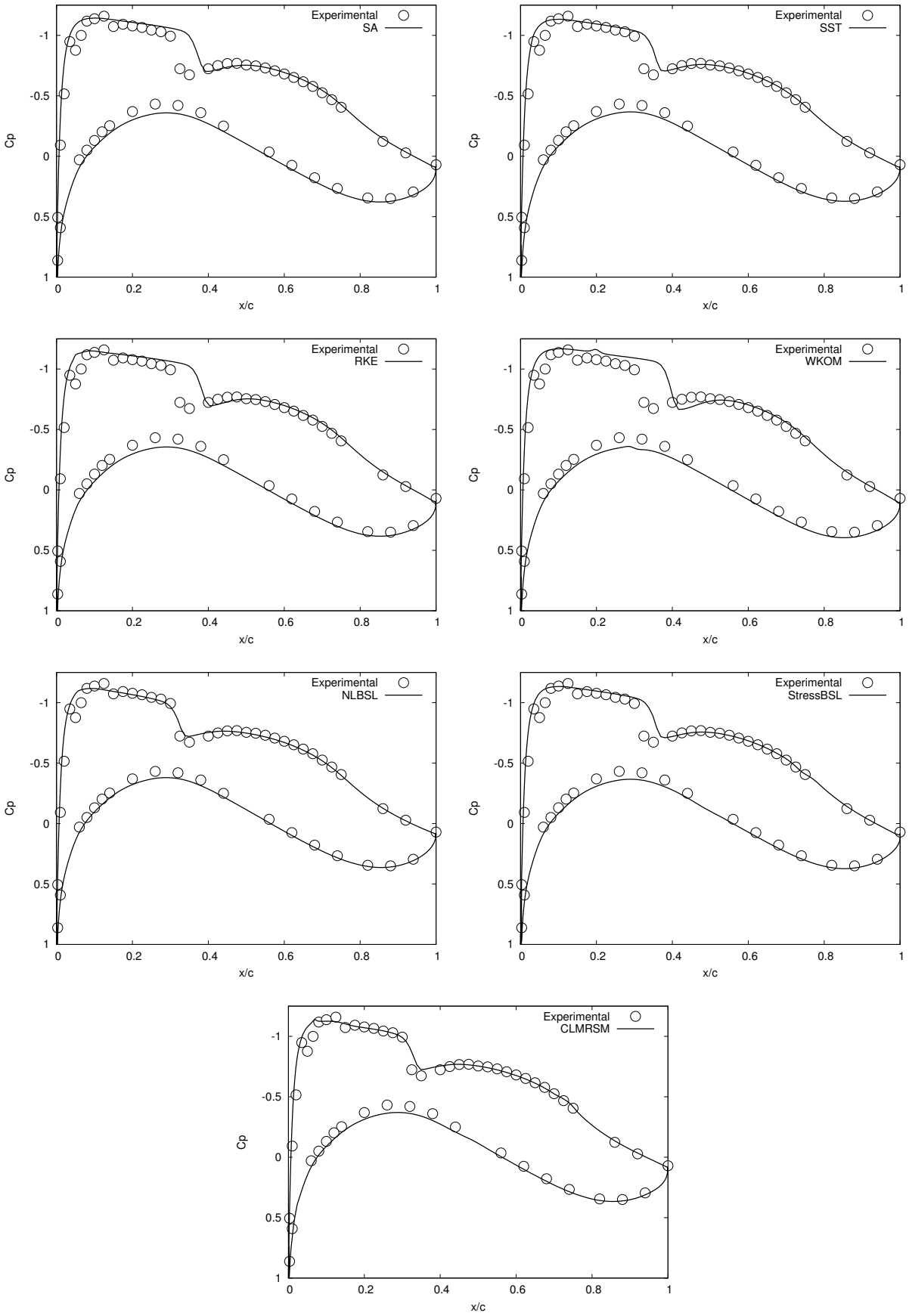

Figure 2: Numerical and experimental Cp distributions for flow conditions $M_\infty = 0.724$, $Re = 3$ million and $\alpha = 1.15$ deg.

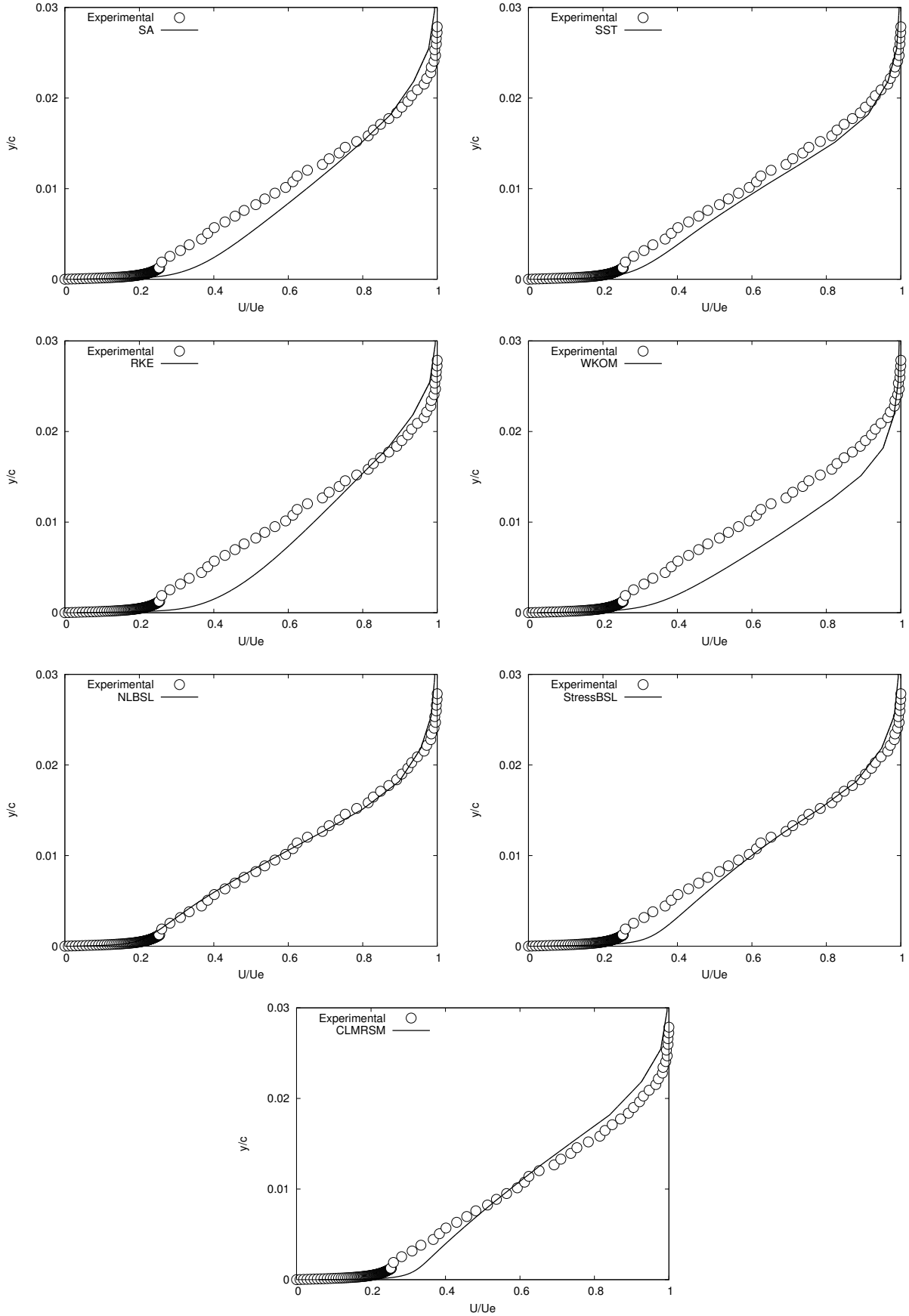

Figure 3: Numerical and experimental boundary layers at $x/c = 95\%$ for flow conditions $M_\infty = 0.724$, $Re = 3$ million and $\alpha = 1.15$ deg.

8. References

Barth, T. J. and Jespersen, D. C., 1989, The Design and Application of Upwind Schemes on Unstructured Meshes, "27th AIAA Aerospace Sciences Meeting", AIAA Paper No. 89-0366, Reno, NV.

Batten, P., Craft, T. J., Leschziner, M. A., and Loyau, H., 1999, Reynolds-Stress-Transport Modeling for Compressible Aerodynamics Applications, "AIAA Journal", Vol. 37, No. 7, pp. 785–796.

Bigarella, E. D. V. and Azevedo, J. L. F., 2005, A Study of Convective Flux Computation Schemes for Aerodynamic Flows, "43rd AIAA Aerospace Sciences Meeting and Exhibit", AIAA Paper No. 2005-0633, Reno, NV.

Bigarella, E. D. V. and Azevedo, J. L. F., 2006, Advanced Eddy-Viscosity and Reynolds-Stress Turbulence Model Simulations of Aerospace Applications, "24th AIAA Applied Aerodynamics Conference", AIAA Paper No. 2006-2826, San Francisco, CA.

Bigarella, E. D. V., Basso, E., and Azevedo, J. L. F., 2004, Centered and Upwind Multigrid Turbulent Flow Simulations with Applications to Launch Vehicles, "22nd AIAA Applied Aerodynamics Conference and Exhibit", AIAA Paper No. 2004-5384, Providence, RI.

Craft, T. J. and Launder, B. E., 1996, A Reynolds Stress Closure for Complex Geometries, "International Journal of Heat and Fluid Flow", Vol. 17, No. 3, pp. 245–254.

Craft, T. J., Launder, B. E., and Suga, K., 1996, Development and Application of a Cubic Eddy-Viscosity Model of Turbulence, "International Journal of Heat and Fluid Flow", Vol. 17, No. 2, pp. 108–115.

Daly, B. and Harlow, F., 1970, Transport Equation in Turbulence, "Physics of Fluids", Vol. 13, pp. 2634–2649.

Fluent, 1998, FIDAP 8 – Tutorial Manual.

Hellsten, A., 2005, New Advanced k-ω Turbulence Model for High-Lift Aerodynamics, "AIAA Journal", Vol. 43, No. 9, pp. 1857–1869.

Johnson, D. A. and King, L. S., 1985, A Mathematically Simple Turbulence Closure Model for Attached and Separated Turbulent Boundary Layers, "AIAA Journal", Vol. 23, No. 11, pp. 1684–1692.

Jones, W. P. and Launder, B. E., 1972, The Prediction of Laminarization with a Two-Equation Model of Turbulence, "International Journal of Heat and Mass Transfer", Vol. 15, No. 2, pp. 301–314.

Kim, J., Moin, P., and Moser, R., 1987, Turbulence Statistics in Fully Developed Channel Flow at Low Reynolds Number, "Journal of Fluid Mechanics", Vol. 177, pp. 133–166.

Launder, B. E., Reece, G. J., and Rodi, W., 1975, Progress in the Development of a Reynolds-Stress Turbulence Closure, "Journal of Fluid Mechanics", Vol. 68, No. 3, pp. 537–566.

Leschziner, M. A. and Drikakis, D., 2002, Turbulence Modelling and Turbulent-Flow Computation in Aeronautics, "The Aeronautical Journal", Vol. 106, No. 1061, pp. 349–383.

Lumley, J. L., 1978, Computational Modeling of Turbulent Flows, Yih, C. -S., editor, "Advances in Applied Mechanics", Vol. 18, pp. 123–176. Academic Press, New York.

Menter, F. R., 1994, Two-Equation Eddy-Viscosity Turbulence Models for Engineering Applications, "AIAA Journal", Vol. 32, No. 8, pp. 1598–1605.

Rodde, A. M. and Archambaud, J. P., 1994, OAT15A Airfoil Data, "A Selection of Experimental Test Cases for the Validation of CFD Codes", number AGARD-AR-303. NATO Advisory Group for Aerospace Research & Development, Case A11.

Roe, P. L., 1981, Approximate Riemann Solvers, Parameter Vectors, and Difference Schemes, "Journal of Computational Physics", Vol. 43, No. 2, pp. 357–372.

Rotta, J., 1951, Statistischer Theorie nichthomogener Turbulenz 1, "Zeitschrift für Physik", Vol. 129, pp. 547–572.

Scalabrin, L. C., 2002, Numerical Simulation of Three-Dimensional Flows over Aerospace Configurations, Master's thesis, Instituto Tecnológico de Aeronáutica, São José dos Campos, SP, Brazil.

Shih, T., Liou, W. W., Shabbir, A., Yang, Z., and Zhu, J., 1994, A New Eddy Viscosity Model for High Reynolds Number Turbulent Flows – Development and Validation, NASA TM 106721, National Aeronautics and Space Administration, Lewis Research Center, Cleveland, Ohio 44135-3191.

Spalart, P. R., 2000, Strategies for Turbulence Modelling and Simulations, "International Journal of Heat and Fluid Flow", Vol. 21, pp. 252–263.

Spalart, P. R. and Allmaras, S. R., 1994, A One-Equation Turbulence Model for Aerodynamic Flow, "La Recherche Aeropastiale", Vol. 1, pp. 5–21.

van Leer, B., 1979, Towards the Ultimate Conservative Difference Scheme. V. A Second-Order Sequel to Godunov's Method, "Journal of Computational Physics", Vol. 32, No. 1, pp. 101–136.

Wallin, S. and Johansson, A. V., 2000, An Explicit Algebraic Reynolds Stress Model for Incompressible and Compressible Turbulent Flows, "Journal of Fluid Mechanics", Vol. 403, pp. 89–132.

Wilcox, D. C., 1998, "Turbulence Modeling for CFD", DCW Industries, La Cañada, CA, second edition.